

# Effect of Selective Enhancement on the Bending Performance of Fused Deposition Methods 3D-Printed PLA Models

Chen Wang,<sup>a,b,\*</sup> Jiahao Yu,<sup>a,b</sup> Minhan Jiang,<sup>a,b</sup> and Jingyao Li<sup>a,b</sup>

The top and bottom shells of fused deposition 3D-printed PLA models are exposed to the highest stresses. To improve the bending performance of PLA models under three-point bending conditions, the models were strengthened by a selective enhancement method. Several sets of PLA models were fabricated using FDM technology, and three-point bending experiments were conducted to compare the bending strength of PLA models when the layer height, top/bottom shell thickness, and extrusion rate were varied. The bending strength of the PLA models increased as the layer height of the top/bottom shell decreased, the thickness increased, and the extrusion rate increased. The average bending strength of the PLA models after selective enhancement was 84.4 MPa, and the average bending modulus of elasticity was 0.816 GPa, which were higher than the average bending strength of 68.6 MPa and the average bending modulus of elasticity of 0.736 GPa of the conventional groups. These results indicated that the selective enhancement method improved the bending performance of 3D-printed PLA models, and it also provided a reference for the improvement of the mechanical properties of the 3D-printed models with cellulose composite reinforced materials.

DOI: 10.15376/biores.19.2.2660-2669

Keywords: Selective enhancement; FDM; PLA models; Bending performance

Contact information: a: College of Furnishings and Industrial Design, Nanjing Forestry University, Nanjing 210037, China; b: Jiangsu Co-Innovation Center of Efficient Processing and Utilization of Forest Resources, Jiangsu, China; \*Corresponding author: 996869559@qq.com

## INTRODUCTION

As the 3D printing continues to improve, models 3D printed by fused deposition methods (FDM) have moved beyond display prototypes. Increasingly, models are involved in the elucidation of mechanisms, which places higher demands on the mechanical performance of the models (Feng *et al.* 2022). Polylactic acid (PLA) is a bio-based and renewable degradable material, and one of the commonly used consumables for FDM 3D printing (Li *et al.* 2022). PLA can be synthesized from material extracted from maize, potato, or starch materials. It can be completely degraded to carbon dioxide and water under industrial composting conditions (Deng *et al.* 2023). PLA has excellent biocompatibility and thermal properties (Zhou *et al.* 2023). In terms of mechanical performance, 3D-printed PLA models have good tensile performance, but the bending performance of 3D-printed PLA models is poor due to the hard texture and poor toughness of PLA, which lacks flexibility and elasticity (Liu *et al.* 2019).

To improve the bending performance of 3D-printed PLA models, a new slicing

process optimisation method, the selective enhancement method, was investigated in this study. This method individually enhances specific regions in 3D-printed PLA models. By changing the slicing parameters of the region, the local and overall structural enhancement of the models can be achieved, thus avoiding the destruction of the models due to excessive local stresses (Liu *et al.* 2020).

In this study, the 3D-printed structural model is decomposed into top shell, bottom shell, bezel and infill structure. Finite element simulation analysis shows that under the three-point bending condition, the bending stress generated in the centre region of the top and bottom shells of the 3D-printed PLA models is the largest. Thus, the selective enhancement is performed on the top and bottom shells of the 3D-printed PLA models to achieve the effective enhancement of the bending performance of the 3D-printed PLA models.

### Selective Enhancement Methods

Slicing is the process of converting a 3D digital model into a machining code by specific parameters through software, and it is also one of the key links in the FDM 3D printing process flow (Mo *et al.* 2022). The selective enhancement method involves the setting of printing parameters for specific regions of the 3D-printed models through the slicing software, which enhances the region as well as the overall structure of the models (Wang *et al.* 2022). This method is suitable for cases in which the loading conditions of the models are known and there are excessive local stresses within the models, such that it is possible to improve the structural strength of the 3D-printed models so that they perform more efficiently and in a more targeted manner (Yang *et al.* 2021).

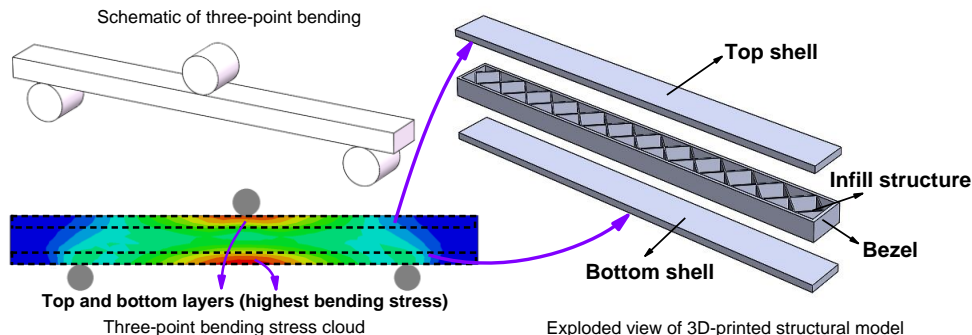


**Fig. 1.** Schematic diagram of selective enhancement methods

As shown in the 3D-printed structural model explosion diagram (Fig. 1), the 3D-printed structural model can be divided into top shell, bottom shell, bezel, and infill structures (Wang *et al.* 2023). In the three-point bending stress cloud diagram (Fig. 1), the top surface of the finite element model is loaded at the midline and causes the overall structure to undergo bending deformation, whereby the inner material of its bending region is compressed along the tangent direction and the outer material is stretched along the tangent direction (Yang *et al.* 2022). The bending stresses generated in the centre region of the top and bottom layers of the finite element model are the greatest, and the damage and destruction leading to the fracture of the model also start from the centre region of the top and bottom layers (Zhou and Xu 2022).

Comparing the 3D-printed structural model and the finite element model of the three-point bending test, the maximum bending stress of the three-point bending finite

element model appeared in the centre region of the top and bottom layers. Thus, it appeared on the top shell and the bottom shell at the corresponding positions of the 3D-printed structural model (Ding *et al.* 2022). Therefore, the top shell and bottom shell of the 3D-printed structural model were set as selective enhancement regions, and the effective enhancement of the bending performance of the 3D-printed PLA models was achieved by changing the printing parameters in this region.

## EXPERIMENTAL

### Materials

The PLA filament (White, 1.75 mm diameter, Miracle 3D, Kunshan, China) was used for additive manufacturing by the FDM. This PLA filament has a melting temperature of 190 °C, a glass transition temperature of 60 °C, and a thermal degradation temperature of 300 °C (Han *et al.* 2022).

### Specimen Preparation

The rectangular model (length, width, and height dimensions: 160 mm\*15 mm\*8 mm) was designed as the specimen for this experiment using SolidWorks software (Dassault Systemes, Education Version 2016, Paris, France), followed by exporting an STL file and importing the STL file into Cura software (Ultimaker, Version 4.2, Gelderland, Netherlands) for slicing. The slicing parameters for the conventional groups (layer height of 0.3 mm, top/bottom shell thickness of 1.2 mm, and extrusion rate of 100%) and the slicing parameters for the selective enhancement groups (parameter settings see below) were set, and the G-code file was exported for 3D printing.

A G-600 3D printer (XYZ printing, 0.4 mm nozzle diameter, Miracle 3D, Kunshan, China) was used for additive manufacturing by the FDM. The main printing parameters were set as follows: the extrusion head temperature was set to 200 °C, the print speed was set to 50 mm/s, the hot bed temperature was set to 60 °C, and the fill pattern was set to grid type (Huang *et al.* 2022).

### Performance Test

The three-point bending performance was measured as shown in Fig. 2. A model with a rectangular cross-section was placed on two supports, and a load was applied to the model by a loading indenter, with the indenter's point of impact at a distance equal to the distance between the two supports (Li *et al.* 2020). Under the bending load, the model deformed in bending. Until the model breaks, the load applied to the specimen by the loading indenter during this process was measured, and bending performance indexes were calculated (Liu *et al.* 2021).

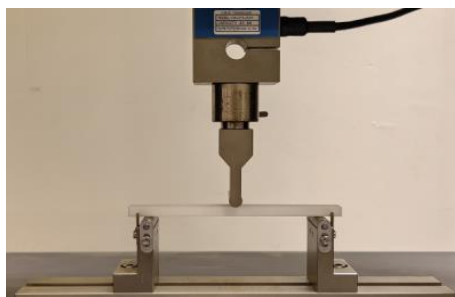


**Fig. 2.** Three-point bending performance test

A universal mechanical testing machine (AG-X, 20 kN, Shimadzu, Kyoto, Japan) was used to test the bending strength of groups of PLA models, and the reference standard was ISO 178-2019. The ambient temperature was 20 °C, the support span was 140 mm, and the loading speed was 2 mm/min (Narlıoğlu 2022).

An industrial flush-focus microscope (CL-MA-48M, Colomer, Guangzhou, China) was used to observe the cross-section morphological features of the PLA models.

## RESULTS AND DISCUSSION

### Effect of Layer Height on Bending Performance of PLA Models

The thickness of the top/bottom shell (selective enhancement region) of the 3D-printed PLA models was set to 1.2 mm, the extrusion rate to 100%, and the layer heights to 0.1, 0.2, and 0.3 mm. To compare the bending strength of the PLA models when the layer heights of the top/bottom shell were different values, 12 tests were conducted on each of the four groups of PLA models, and the results of the tests are shown in Fig. 3. The mean value of the bending strength of the PLA models increased as the layer height of the top/bottom shell decreased in the range of 0.1 to 0.3 mm. This is because as the layer height decreases, the extrusion pressure of the 3D printer nozzle in the vertical direction increases, which makes the molten filament fully extruded at the interlayer adhesion interface (Qi *et al.* 2023). This extrusion increases the bonding area of the contact surfaces of neighboring filaments, and it also promotes the infiltration and diffusion of the polymer molecules, which effectively improves the interlayer adhesion strength of the top/bottom shell (Wang *et al.* 2019). With the increase of interlayer bonding strength, the PLA models were more resistant to bending damage.

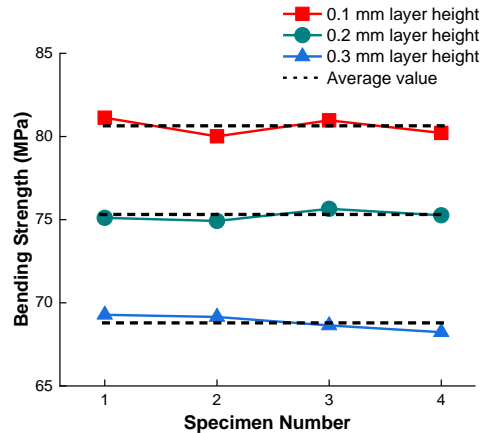


Fig. 3. Effect of layer height on the bending strength of PLA models

### Effect of Top/Bottom Shell Thickness on Bending Performance of PLA Models

The layer height of the top/bottom shell (selective enhancement region) of the 3D-printed PLA models was set to 0.3 mm, the extrusion rate to 100%, and the thicknesses to 1.2, 1.5, and 1.8 mm. To compare the bending strength of the PLA models when the thicknesses of the top/bottom shell were of different values, 12 tests were carried out for each of the four groups of PLA models, and the results of the tests are shown in Fig. 4. The average value of the bending strength of the PLA models increased as the thickness of the top/bottom shell increased in the range of 1.2 to 1.8 mm. The overall thickness of the 3D-printed PLA models is equal to the sum of the top/bottom shell thickness and the thickness of the infill structure. As the thickness of the top/bottom shell increased, the thickness of the infill structure decreased accordingly (Wang *et al.* 2020). Unlike the low-density cross-thin-wall layout of the infill structure, the top/bottom shell was solid, which resulted in an increase in the load-bearing area of the top/bottom shell. A smaller load per unit area results in a smaller the bending stress value and better ability to resist damage (Yee *et al.* 2016). Therefore, as the thickness of the top/bottom shell increased, the ability of the PLA models to resist bending damage increased.

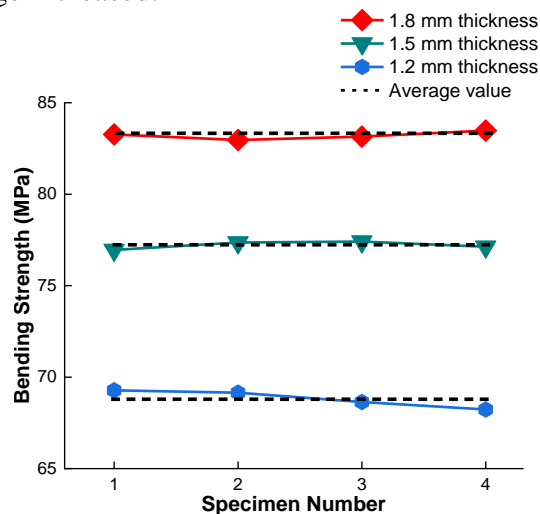
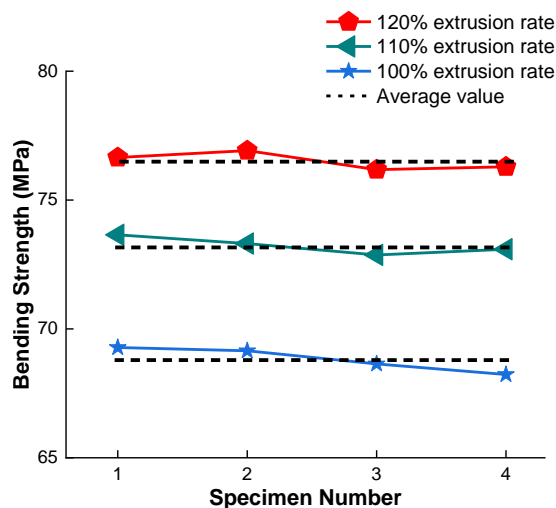


Fig. 4. Effect of top/bottom shell thickness on the bending strength of PLA models

### Effect of Extrusion Rate on the Bending Performance of PLA Models

The layer height of the top/bottom shell (selective enhancement region) of the 3D-printed PLA models was set to 0.3 mm, thickness to 1.2 mm, and extrusion rates of 100%, 110%, and 120%. To compare the bending strength of the PLA models when the extrusion rate of the top/bottom shell was different values, 12 tests were carried out for each of the four groups of PLA models, and the test results are shown in Fig. 5.



**Fig. 5.** Effect of extrusion rate on the bending strength of PLA models

The mean value of the bending strength of the PLA models increased as the extrusion rate of the top/bottom shell increased in the range of 100% to 120%. Due to the elliptical structure of the viscous fluidic filaments extruded by the FDM technology, pores usually are present at the combination of their vertical neighbors and transverse filaments (Zhou *et al.* 2020). Under the influence of bending stress, the stress concentration tends to occur at the pores, often leading to cracking, which is the main reason for the bending damage of the PLA models. With the increase of extrusion rate, the extruded amount of filaments per unit time increased. The increased filaments flowed and filled the pore defects, which reduced the stress concentration and improved the bending strength of the PLA models.

### Comparative Analysis of Selective Enhancement Effects

Based on the experimental results described above, the layer height of 0.1 mm, top/bottom shell thickness of 1.8 mm, and extrusion rate of 120% are the optimal parameters for each group of experiments, which all make the bending strength of the selectively enhanced PLA models effectively improved. To verify the effect of selective enhancement of PLA models, the above three groups of parameters (layer height 0.1 mm, top/bottom shell thickness 1.8 mm, extrusion rate 120%) were selected as the parameter combinations to print three groups of PLA models (enhanced group 1, 2, 3), respectively, and compared with three groups of PLA models without selective enhancement (conventional group 4, 5, 6). The results are shown in Fig. 6.

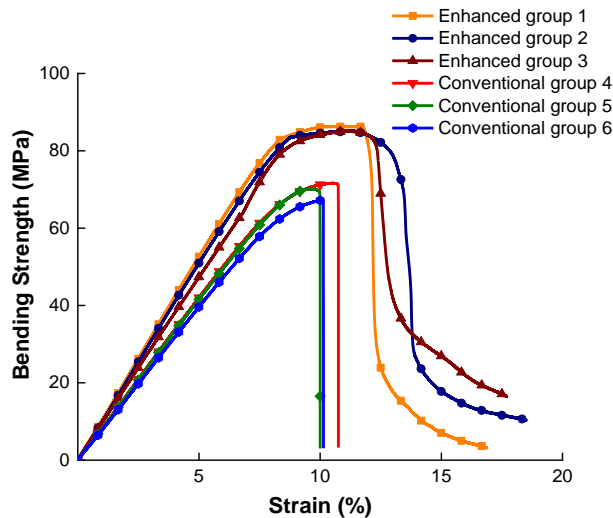


Fig. 6. Stress-strain curves

The average bending strength of the PLA models after selective enhancement was 84.4 MPa, and the average bending elastic modulus is 0.816 GPa, which are higher than the average bending strength of 68.6 MPa and the average bending elastic modulus of 0.736 GPa of the conventional group. These results indicated that selective enhancement method achieved an effective enhancement of the bending performance of the 3D-printed PLA models. Observing the micro-morphological characteristics of the fracture site of the three-point bending models (shown in Fig. 7), the fracture site of the PLA models in the conventional groups showed brittle fracture characteristics, and the fracture surface was smooth. The fracture site of the PLA models after selective enhancement showed toughness fracture characteristics, and the fracture surface was rough. There were many filaments that were not completely disconnected, indicating that the selective enhancement method effectively improved the bending toughness of the PLA models. This was due to the increased volume of the solid structure in the PLA model after selective enhancement, and this solid structure, which was made of dense stacks of fused filaments bonded together, had a better load-bearing capacity and fracture toughness than the low-density infill structure outside the selective enhancement region, and thus could effectively improve the bending toughness of the PLA models. In addition, as seen from the comparison of the bending strength values between the three enhanced groups and the three conventional groups, the experimental results (bending strength) had a certain degree of dispersion, which may be related to the stress concentration damage caused by the presence of some crack defects in the 3D-printed PLA models.

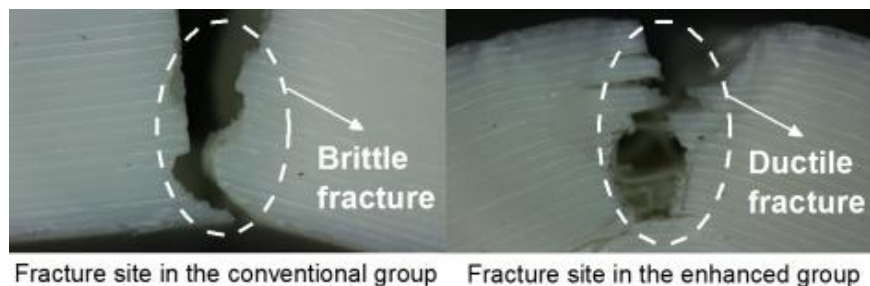


Fig. 7. Micro-morphological of the fracture site

## POSSIBLE FUTURE WORK

With the continuous development of 3D-printed materials, cellulose and its derivatives have been gradually applied to the preparation of 3D-printed materials and the improvement or enhancement of the performance of printed products. In this study, the authors have effectively improved the bending performance of 3D-printed PLA models by selective enhancement methods. It is hoped to extend this research idea to cellulose-based 3D-printed materials. The objective of such work would be to analyze the methods of enhancing the mechanical performance of cellulose-based 3D-printed models and to attempt to improve the mechanical performance of cellulose-based 3D-printed models by using selective enhancement methods.

## CONCLUSIONS

1. The bending strength of the PLA models increases as the layer height of the top/bottom shell decreases, the thickness increases, and the extrusion rate increases. The average bending strength of the PLA models after selective enhancement was 84.4 MPa and the average bending elastic modulus was 0.816 GPa, which are higher than the average bending strength of 68.56 MPa and the average bending elastic modulus of 0.736 GPa of the conventional group, indicating that selective enhancement method can achieve the effective enhancement of the bending performance of the 3D-printed PLA models.
2. The fracture site of the PLA models in the conventional groups showed brittle fracture characteristics, while the fracture site of the PLA models after selective enhancement showed toughness fracture characteristics, indicating that the selective enhancement method effectively improved the bending toughness of the PLA models.

## REFERENCES CITED

- Deng, J.-Z., Huang, N., and Yan, X.-X. (2023). "Effect of composite addition of antibacterial/photochromic/self-repairing microcapsules on the performance of coatings for medium-density fiberboard," *Coatings* 13(11), article 1880. DOI: 10.3390/coatings13111880
- Ding, T.-T., Yan, X.-X., and Zhao, W.-T. (2022). "Effect of urea–formaldehyde resin–coated colour–change powder microcapsules on performance of waterborne coatings for wood surfaces," *Coatings* 12(9), article 1289. DOI: 10.3390/coatings12091289
- Feng, X.-H., Yang, Z.-Z., Wang, S.-Q., and Wu, Z.-H. (2022). "The reinforcing effect of lignin-containing cellulose nanofibrils in the methacrylate composites produced by stereolithography," *Polymer Engineering and Science* 2022(9), 2968-2976. DOI: 10.1002/pen.26077
- Han, Y., Yan, X.-X., and Zhao, W.-T. (2022). "Effect of thermochromic and photochromic microcapsules on the surface coating properties for metal substrates," *Coatings* 12(11), article 1642. DOI: 10.3390/coatings12111642
- Huang, N., Yan, X.-X., and Zhao, W.-T. (2022). "Influence of photochromic microcapsules on properties of waterborne coating on wood and metal substrates," *Coatings* 12(11), article 1750. DOI: 10.3390/coatings12121857

- Li, R.-R., Chen, J.-J., and Wang, X.-D. (2020). "Prediction of the color variation of moso bamboo during CO<sub>2</sub> laser thermal modification," *BioResources* 15(3), 5049-5057. DOI: 10.15376/biores.15.3.5049-5057
- Li, W.-B., Yan, X.-X., and Zhao, W.-T. (2022). "Preparation of crystal violet lactone complex and its effect on discoloration of metal surface coating," *Polymers* 14(20), 4443. DOI: 10.3390/polym14204443
- Liu, Q., Gu, Y., Xu, W., Lu, T., Li, W., and Fan, H. (2021). "Compressive properties of green velvet material used in mattress bedding," *Applied Sciences* 11(23), article 11159. DOI:10.3390/app112311159
- Liu, X.-Y., Lv, M.-Q., Liu, M., and Lv, J.-F. (2019). "Repeated humidity cycling's effect on physical properties of three kinds of wood-based panels," *BioResources* 14(4), 9444-9453. DOI: 10.15376/biores.14.4.9444-9453
- Liu, Y., Hu, J., and Wu, Z.-H. (2020). "Fabrication of coatings with structural color on a wood surface," *Coatings* 10(1), article 32. DOI: 10.3390/coatings10010032
- Mo, X.-F., Zhang, X.-H., Fang, L., and Zhang, Y. (2022). "Research progress of wood-based panels made of thermoplastics as wood adhesives," *Polymers* 14(1), article 98. DOI: 10.3390/polym14010098
- Narlıoğlu, N. (2022). "Comparison of mechanical properties of 3D-printed and compression-molded wood-poly(lactic acid) (PLA) composites," *BioResources* 17(2), 3291-3302. DOI: 10.15376/biores.17.2.3291-3302
- Qi, Y.-Q., Sun, Y., Zhou, Z.-W., Huang, Y., Li, J.-X., and Liu, G.-Y. (2023). "Response surface optimization based on freeze-thaw cycle pretreatment of poplar wood dyeing effect," *Wood Research* 68(2), 293-305. DOI: 10.37763/wr.1336-4561/68.2.293305
- Wang, X.-H., Wu, Y., Chen, H., Zhou, X.-Y., Zhang, Z.-K., and Xu, W. (2019). "Effect of surface carbonization on mechanical properties of LVL," *BioResources* 14(1), 453-463. DOI: 10.15376/biores.14.1.453-463
- Wang, S., Chen, L., Xu, L.-J., Guan, H., Yan, S., and Wu, Z.-H. (2020). "Comparative study on the tensile performance of box frames constructed by keyed joints and dovetail joints," *BioResources* 15(4), 9291-9302. DOI: 10.15376/biores.15.4.9291-9302
- Wang, L., Han, Y., and Yan, X.-X. (2022). "Effects of adding methods of fluorane microcapsules and shellac resin microcapsules on the preparation and properties of bifunctional waterborne coatings for basswood," *Polymers* 14(18), 3919. DOI: 10.3390/polym14183919
- Wang, Q., Feng, X.-H., and Liu, X.-Y. (2023). "Functionalization of nanocellulose using atom transfer radical polymerization and applications: A review," *Cellulose* 30, 8495-8537. DOI: 10.1007/s10570-023-05403-5
- Yang, L., Han, T.-Q., Liu, Y.-X., and Yin, Q. (2021). "Effects of vacuum heat treatment and wax impregnation on the color of *Pterocarpus macrocarpus* Kurz," *BioResources* 16(1), 954-963. DOI: 10.15376/biores.16.1.954-963
- Yang, Z.-Z., Feng, X.-H., Xu, M., and Rodrigue, D. (2022). "Printability and properties of 3D printed poplar fiber/poly(lactic acid) biocomposites," *BioResources* 16(2), 2774-2788. DOI: 10.15376/biores.16.2.2774-2788
- Yee, Y.-Y., Ching, Y.-C., Rozali, S., Awanis Hashim, N., and Singh, R. (2016). "Preparation and characterization of poly(lactic acid)-based composite reinforced with oil palm empty fruit bunch fiber and nanosilica," *BioResources* 11(1), 2269-2286. DOI: 10.15376/biores.11.1.2269-2286

- Zhou, C.-M., Huang, T., and Liang, S. (2020). "Smart home R&D system based on virtual reality," *Journal of Intelligent & Fuzzy Systems* 40(2), 3045-3054. DOI: 10.3233/jifs-189343
- Zhou, C.-M., Huang, T., Luo, X., and Kaner, J. (2023). "Reorganisation and construction of an age-friendly smart recreational home system: based on function-capability match methodology," *Applied Sciences-Basel* 13(7), article 9783. DOI: 10.3390/app13179783.
- Zhou, J.-C., and Xu, W. (2022). "Toward interface optimization of transparent wood with wood color and texture by silane coupling agent," *Journal of Materials Science* 57(10), 5825-5838. DOI: 10.1007/s10853-022-06974-7

Article submitted: January 31, 2024; Peer review completed: February 17, 2024; Revised version received and accepted: February 25, 2024; Published: March 7, 2024.  
DOI: 10.15376/biores.19.2.2660-2669